AD-A148 571 POLY(DIMETHYLSILOXANE)-POLYURETHANE ELASTOMERS: 1/1
SYNTHESIS AND PROPERTIES O..(U) WISCONSIN UNIV-MADISON
DEPT OF CHEMICAL ENGINEERING Y XUEHAI ET AL. NOV 84
UNCLASSIFIED N00014-83-K-0423 F/G 11/10 NL

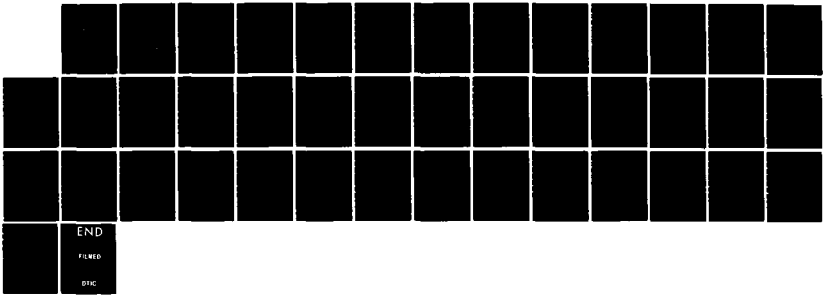

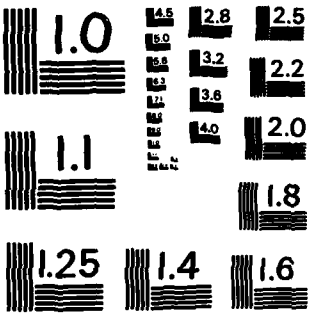

SECURITY CLASSIFICATION

REPORT

AD-A148 571

READ INSTRUCTIONS BEFORE COMPLETING FORM

1. REPORT NUMBER
5

3. RECIPIENT'S CATALOG NUMBER

4. TITLE (and Subtitle)
Poly(dimethylsiloxane)-Polyurethane Elastomers: Synthesis and Properties of Segmented Copolymers and Related Zwitterionomers

5. TYPE OF REPORT & PERIOD COVERED
Interim Technical Report

6. PERFORMING ORG. REPORT NUMBER

7. AUTHOR(s)
Yu Xuehai, M. R. Nagarajan, T. G. Grasel, P. E. Gibson and S. L. Cooper.

8. CONTRACT OR GRANT NUMBER(s)
N00014-83-K-0423

9. PERFORMING ORGANIZATION NAME AND ADDRESS
Department of Chemical Engineering
University of Wisconsin
Madison, WI 53706

10. PROGRAM ELEMENT, PROJECT, TASK AREA & WORK UNIT NUMBERS

11. CONTROLLING OFFICE NAME AND ADDRESS
Department of the Navy
Office of Naval Research
Arlington, Virginia 22217

12. REPORT DATE
Nov. 1, 1984

13. NUMBER OF PAGES
21

14. MONITORING AGENCY NAME & ADDRESS(if different from Controlling Office)

15. SECURITY CLASS. (of this report)
Unclassified

15a. DECLASSIFICATION/DOWNGRADING SCHEDULE

16. DISTRIBUTION STATEMENT (of this Report)
Distribution unlimited

17. DISTRIBUTION STATEMENT (of the abstract entered in Block 20, if different from Report)

DTIC ELECTE DEC 7 1984 S A

18. SUPPLEMENTARY NOTES
To be published in Journal of Polymer Science- Physics

19. KEY WORDS (Continue on reverse side if necessary and identify by block number)
Polymethylsiloxane, polyurethane, elastomers, ionomers

20. ABSTRACT (Continue on reverse side if necessary and identify by block number)

A series of polyurethane block polymers based on hydroxybutyl-terminated poly(dimethylsiloxane) soft segments of molecular weight 2000 were synthesized. The hard segments consisted of 4,4'-methylenediphenylene diisocyanate (MDI) which was chain extended with either 1,4-butanediol (BD) or N-methyldiethanolamine (MDEA). The MDEA-extended materials were ionized using 1,3-propane sultone. The weight fraction of hard segments was in range 0.13-0.39. The morphology and properties of these polyurethane elastomers were studied by a variety of

Cont.

DD FORM 1 JAN 73 1473 EDITION OF 1 NOV 65 IS OBSOLETE

S/N 0102-LF-014-6601

SECURITY CLASSIFICATION OF THIS PAGE (When Data Entered)

FILE COPY

20. Abstract (cont.)

techniques. All of these short segment block copolymers showed nearly complete phase separation. The zwitterionomer materials exhibited ionic aggregation within the hard domains. Hard segment crystallinity or ionic aggregation did not affect the morphology. Hard domain cohesion was found to be a more important factor than hard domain volume fraction in determining the tensile and viscoelastic properties of these elastomers.

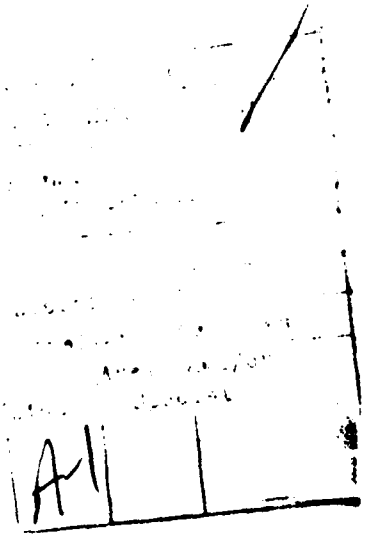

OFFICE OF NAVAL RESEARCH

Contract N00014-83-K-0423

TECHNICAL REPORT NO. 5

Poly(dimethylsiloxane)-Polyurethane Elastomers: Synthesis and Properties of Segmented Copolymers and Related Zwitterionomers

by

Yu Xuehai, M. R. Nagarajan, T. G. Grasel, P. E. Gibson

and S. L. Cooper

Prepared for Publication

in the

Journal of Polymer Science-Physics

Department of Chemical Engineering
University of Wisconsin
Madison, Wisconsin 53706

November 1984

I. INTRODUCTION

Thermoplastic polyurethane elastomers are block copolymers of the $(A-B)_n$ type, consisting of alternating soft and hard segments. At service temperatures the soft segment is in a viscous or rubbery state, while the hard segment is in a glassy or semicrystalline state. The soft segment provides elastomeric character to the polymer, while the hard segment provides dimensional stability by acting as a thermally reversible and multifunctional crosslink and also as a reinforcing filler. The unusual properties of these copolymers are directly related to their two-phase structure.

In conventional segmented linear polyurethanes the soft segments are commonly low molecular weight (600-3000) polyether or polyester macroglycols while the hard segments usually consist of an aromatic diisocyanate which is chain extended with a low molecular weight diol to produce blocks with a range of molecular weights. The driving force for phase separation in these systems is the incompatibility of the two segment types. A wide spectrum of physical properties and morphologies has been observed, depending upon the composition and chemical architecture of the hard and soft segments (1-6).

The incorporation of low molecular weight poly(dimethylsiloxane) as a soft segment material to produce a polyurethane block copolymer gives materials with interesting bulk and surface properties due to the characteristics of the siloxane soft segment (7). These characteristics include a wide service temperature range due to the very low poly(dimethylsiloxane) glass transition temperature (-123°C), good thermal and oxidative stability, increased impact strength, good release properties,

incompatibility with most organic compounds, and excellent electrical insulating properties. Due to their low surface energy, the siloxane segments tend to migrate to the air-polymer interface and provide a very hydrophobic surface (8,9). Siloxanes are also of interest as possible biomaterials (10-11), and the oxygen permeability that has been observed in poly(dimethylsiloxane) systems is also of interest (12). Poly(dimethylsiloxanes) are physiologically inactive, very low in toxicity and present no health hazards. Thus, siloxane-containing copolymers should find a wide range of potential applications as elastomers, coatings, biomaterials, and environmentally stable compounds.

Poly(dimethylsiloxane)-polyurethane materials are likely to be highly phase separated due to the large differences in the soft and hard segment solubility parameters and also the lack of hard segment-soft segment hydrogen bonding. Similar characteristics have also been noted for poly(butadiene) and poly(isobutylene) polyurethanes (13,14).

One method used to enhance the degree of phase separation in polyurethane block copolymer is the introduction of ionic centers in the hard segment units. In previous studies of polyurethane zwitterionomers (15-18), materials incorporating N-methyl-diethanolamine (MDEA) as the hard segment chain extender were synthesized and their properties studied. Ionization was accomplished by quaternization of the tertiary amine of MDEA by reaction in solution with 1,3-propane sultone. These studies of polyether-polyurethane zwitterionomers found that ion incorporation increased phase separation and hard domain cohesion. This is caused by a clustering of the ionic groups which also gives rise to an enhancement of mechanical properties.

The synthesis of poly(dimethylsiloxane)-based polyurethanes suffers from problems related to the solubility of various components of the

poly(siloxane-urethane) in the reaction medium due to their large solubility differences. This makes the selection of a suitable solvent difficult. Recently, Yilgör et al. (19) studied the kinetics of a model system of poly(urethane-siloxane) copolymers. To our knowledge, the chain extended poly(dimethylsiloxane)-urethanes have not been studied in detail.

In this investigation, a series of poly(dimethylsiloxane)-polyurethanes were synthesized, and the effect of the degree of ionization on the physical properties was explored. The hard segments consisted of 4,4'-diphenylmethane diisocyanate (MDI) and either 1,4 butanediol (BD) or N-methyldiethanolamine (MDEA) as the chain extender. The zwitterionomers were based on MDI/MDEA hard segments. The soft segment material was a hydroxy-terminated poly(dimethylsiloxane) of molecular weight 2000. Different molar ratios of hard segment to chain extender to soft segment based on both BD and MDEA were prepared. The purpose of this work was to investigate the effect of different chain extenders and zwitterionization on the microphase morphology and physical properties.

II. EXPERIMENTAL ASPECTS

A. Synthesis of Materials

1,3-bis(4-hydroxybutyl)tetramethyldisiloxane (HT) (Silar Laboratories, Inc.) was used without purification. Octamethylcyclotetrasiloxane (D_4) (Petrarch Systems, Inc.) was distilled before use and dried over 4 Å molecular sieves. The 4,4'-diphenylmethane diisocyanate (MDI) (Polysciences) was melted and pressure filtered at 60°C and subsequently precipitated in hexane in an ice bath, while the 1,4-butanediol (BD) (Aldrich) and N,N-dimethylacetamide (DMAC) (Aldrich) were dehydrated over calcium hydride for two days and then vacuum distilled. Tetrahydrofuran

(Aldrich) was dehydrated over calcium hydride. N-methyldiethanolamine (MDEA) (Aldrich) at 97 percent purity, stannous octoate catalyst (M&T Chemicals), and triethylamine (Eastman) were used as received.

The hydroxybutyl terminated poly(dimethylsiloxane) (HTPS-2000) macroglycol was made by reacting 27.9 g (0.1 mole) of 1,3-bis(4-hydroxybutyl)-tetramethyldisiloxane and 178 g. (0.6 mole) of octamethylcyclotetrasiloxane in a reaction flask equipped with a magnetic stirrer, reflux condenser, thermometer and nitrogen inlet tube. About 0.1 weight percent of tetramethyl ammonium hydroxide (Aldrich) was added and the flask was heated to 80°C in a nitrogen atmosphere. About five minutes after the catalyst was added, the viscosity of the reaction mixture increased and the fluid became clear. The reaction was followed by measuring the viscosity (relative flow times) as a function of time, while stirring the reactants at 80°C. A plot of relative viscosity versus time is shown in Figure 1. After 10 hours, the product was heated to 140-145°C for an hour to decompose the catalyst. Unreacted cyclic siloxanes were then removed by vacuum distillation (< 20 mm Hg) at 130°C. Gel permeation chromatography showed that no monomer was present. The molecular weight was checked by using the H^1 NMR CH_2/CH_3 ratio. The HTPS-2000 macroglycol had a number average molecular weight of 1998.

The segmented poly(dimethylsiloxane)-polyurethanes used in this study were synthesized by the two-step condensation reaction shown in Scheme 1. Solutions of HTPS-2000 and MDI were prepared in a mixed solvent system of 3:1 v/v of tetrahydrofuran to N,N'-dimethylacetamide. The HTPS solution, containing 0.15 percent stannous octoate and triethylamine (unnecessary in the MDEA series) as catalysts, was added to the stirred MDI solution in

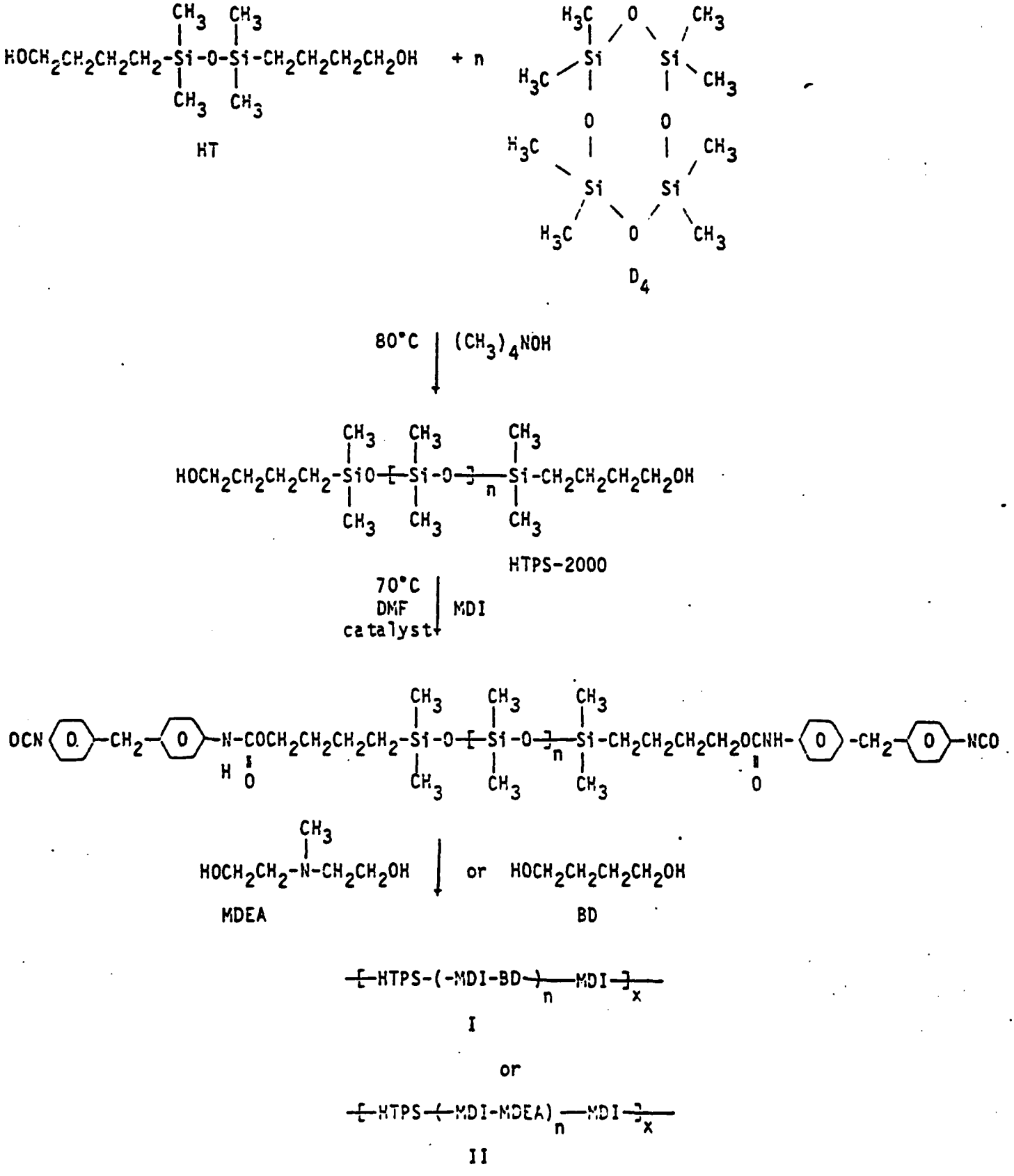

Scheme 1. Synthetic scheme for polysiloxane-polyurethane.

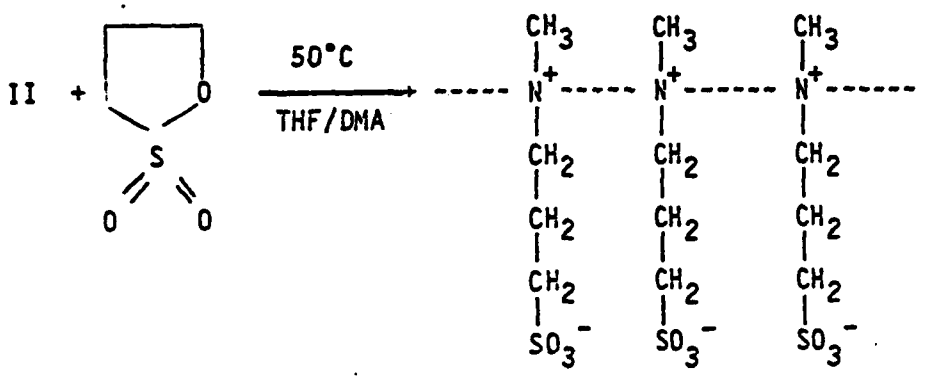

Scheme 2. Synthetic scheme for zwitterionization of MDI/MDEA/HTPS polymer.

several parts at 60-70°C under dry nitrogen. After an hour, the chain extender was added, and stirring was continued in the same temperature range. Chain extension with butanediol and MDEA required 6 hours and 30 minutes, respectively. After GPC verification that a satisfactory molecular weight had been achieved, the polymer was precipitated in hot water, washed with ethyl alcohol, and then dried in a vacuum oven at 70-80°C for at least two days. The yield of polymer in all cases was greater than 95%. The soft segment analog (MDI:HTPS 1:1) was synthesized by a similar procedure.

Zwitterionization was carried out on a portion of the MDEA-extended polymers by first dissolving them in the aforementioned mixed solvent of THF and DMAC. A stoichiometric amount of 1,3-propane sultone (Aldrich) was added, and the reaction mixture was stirred at 40°-50°C for 3 hours. This reaction is shown in Scheme 2. GPC indicated that the reaction did not cause any change in the molecular weight distribution of the polymer.

All materials studied are described in Table 1. A polymer made from one mole of 2000 MW hydroxy-terminated poly(dimethylsiloxane) (HTPS), 3 moles of MDI and 2 moles of MDEA is designated as HTPS-25-0. The code indicates that this polymer contains 25 weight percent MDI and has a HTPS-2000 soft segment and zero % ionization. The polymer HTPS-25-5.0 has been completely reacted with 1,3-propane sultone and contains 5.0 weight percent SO_3 (or 7.6 weight percent of 1,3-propane sultone).

5. Test Methods

Films of block copolymers were spin cast from a solvent mixture of THF and DMA in a 3 to 1 volume ratio, dried in a vacuum oven at 55°C for one week, and then stored in a desiccator at room temperature. Film thicknesses

ranged from 5 μm to 200 μm depending upon the test and test conditions. All films were transparent to visible light.

The molecular weights of the polymers were obtained by passing one percent (w/v) THF solutions through a Waters Associates Model 501 high pressure chromatograph. The average molecular weights were calculated on the basis of the molecular weight vs. retention volume curve of monodisperse polystyrene standards.

Infrared survey spectra were recorded with a Nicolet 7199 Fourier transform infrared spectrophotometer operated with a dry air purge. One hundred scans at a resolution of 2 cm^{-1} were signal-averaged before Fourier transformation.

Thermal analysis was carried out on a Perkin-Elmer DSC-2C interfaced with a Model 3600 Data Station using TADS software. Temperature and enthalpy calibration were carried out using indium and mercury as standards. A heating rate of 20°K/min under a He purge was used on samples of 10 ± 3 mg. The data processing unit allowed automatic subtraction of the base line and normalization of the thermogram for the sample weight.

Dynamic mechanical data were obtained using a Rheovibron DDV-II apparatus which was controlled by a computer. All measurements were carried out under a nitrogen purge at a frequency of 110 Hz with a constant heating rate of 2°K/min.

Room temperature uniaxial stress-strain data were taken on an Instron table model tensile device at a crosshead speed of 0.5 in/min. Dumbbell-shaped samples with a gauge length of 1.5 inches were stamped out with an ASTM 412-D die.

Small-angle x-ray scattering (SAXS) experiments were carried out using a rotating anode x-ray generator operating at 40 kV accelerating

potential and 50 mA emission current. A nickel filter was used to select Cu K_α x-rays (λ = 0.1542 nm) as the primary wavelength. A modified Kratky compact SAXS camera was used to collimate the x-rays into a beam which was about 1.25 cm by 100 μm at the sample. The collimation optics, the sample holder, and the enclosed scattering path were evacuated to eliminate scattering by air. The sample-to-detector distance was approximately 0.6 meters. Scattered x-rays were detected by a one-dimensional position-sensitive detector and associated electronics. The SAXS data were collected by a multi-channel analyzer and transferred to a computer for subsequent analysis. Corrections were made to the data to take into account the detector sensitivity, the detector dark current, parasitic scattering, and sample absorption. Relative intensity data were converted to absolute intensity data by using a Lupolen (polyethylene) standard (20). In order to eliminate slit-length smearing effects, an experimentally measured slit-length weighting function was used to desmear the data by the iterative method of Lake (21).

III. RESULTS AND DISCUSSION

A. Synthesis

The anionic catalyst attacks both D_4 (ring) and HT (linear chain) during the polymerization. The competing reactions are:

$$-D_x- + D_4 \longrightarrow -D_{(x+4)}- \quad (1)$$

$$-D_x- + MM \longrightarrow MD_xM \quad (2)$$

$$MD_xM + MM \longrightarrow MD_{(x-y)}M + MD_yM \quad (3)$$

$$MD_xM + MD_yM \longrightarrow MD_{(x+w)}M + MD_{(y-w)}M \quad (4)$$

If the process represented by reaction (1) is faster than the others, it would cause a viscosity peak during the early stage of the polymerization as in the case of hexamethyldisiloxane equilibration with D_4 [22].

The viscosity-time relationship of the HTPS synthesis is shown in Figure 1. The shape of the curve indicates an approximately equal reactivity of D_4 and HT towards the alkaline catalyst. This could be because the hydroxy group, with its electron donating ability, has an accelerating effect on the cleavage of the Si-O bond of HT.

The critical step of the polymer synthesis is the choice of the reaction solvents, because of the large solubility parameter differences between siloxane and urethane components. It was found that a 3:1 ratio of THF to DMAC could be used satisfactorily to prepare all seven samples. However, it is difficult to use this solvent mixture to synthesize poly(dimethylsiloxane) block copolymers with higher hard segment content than those examined in this study.

Ionic groups are present in the MDEA-extended materials after zwitterionization in solution. During the spin casting of the ionized polymer solution, it is expected that the ionic groups aggregate. Ionic aggregates are expected to have a high binding energy so that once the aggregates have formed it should be very difficult to redissolve the materials under the same conditions (temperature and solvent) used for spin casting. After spin casting, the ion-containing MDEA-extended materials could not be dissolved. We take this observation as strong evidence that ionic aggregation occurs in polyurethane zwitterionomer block polymers.

B. Infrared Spectroscopy

Hydrogen bonding between the urethane hard segment and the siloxane soft segment does not occur because there are no proton donors or acceptors in the siloxane soft segment (bonding to the siloxane oxygen is restricted by steric hindrance). Thus, hydrogen bonding occurs only in the hard domains

with NH hydrogen atoms functioning as donors and the C=O bonds serving as proton acceptors. A typical survey infrared spectrum of a poly(dimethylsiloxane)-polyurethane block copolymer (Sample HTPS-20) is shown in Figure 2. The bands near 3300 cm^{-1} (N-H stretch), 1700 cm^{-1} (C=O stretch), 1540 cm^{-1} (C-N-H bending) and 1280 cm^{-1} (N-C-O stretch) are typical of polyurethane hard segments. The presence of the peaks at 1252 cm^{-1} (sym CH_3 bending), 1060 cm^{-1} (Si-O-Si) stretch, and 842 and 794 cm^{-1} (CH_3 rocking) indicates the inclusion of the siloxane chains in the final polymer. The assignments of IR bands in this work agree with those of Yilgör et al. (19).

Figure 3 shows the IR spectra of four materials in the NH and C=O stretching region. Based on the NH band in the region of 3200-3500 cm^{-1}, the HTPS-10 material appears to be primarily hydrogen bonded, because the bonded NH peak at 3310 cm^{-1} predominates, while the free (non-hydrogen-bonded) NH peak at 3460 cm^{-1} is detectable only as a very small shoulder. In the carbonyl region between 1650-1750 cm^{-1}, the peak due to bonded C=O stretching centered at 1700 cm^{-1} predominates, and that due to free C=O stretching appears as a shoulder at 1730 cm^{-1}. Assuming that the extinction coefficient of free and bonded C=O are the same in polyurethanes (23,24), the dominance of the bonded C=O peak indicates that a large fraction of the hard segments are hydrogen-bonded. This inter-urethane bonding is considered to occur in the interior of the hard domains.

The IR spectra of the BD-extended materials, HTPS-20 and HTPS-25, which are presented in Figures 2 and 3, are very similar and indicate that nearly all the NH and C=O groups are bonded. IR spectra like these are expected for highly phase-separated polyurethanes (26). It should be noted that the

bonded NH and C=O peaks are broader for the low hard segment content material, HTPS-10, than for the higher hard segment content materials, HTPS-20 and HTPS-25. Increasing the hard segment content gives larger hard domains which have more inter-urethane bonding. In addition, because the MDI/BD hard segments are crystallizable, increasing hard segment content allows greater hard domain packing order and thus more uniformity in the inter-urethane bonding energy.

The IR spectra of the MDEA-extended materials, HTPS-25-0.0 and HTPS-25-5.0, are shown in Figure 3. Just as the BD-extended materials, the MDEA-extended materials show negligible amounts of free NH or C=O groups which indicates that these materials are highly phase-separated. There is a noticeable difference between the IR spectra of the BD-extended and the MDEA-extended materials - the MDEA-extended materials have broader NH and C=O peaks and the peaks have a larger area. We interpret the peak broadening to indicate that the MDEA-based hard segments have a lower degree of packing order and thus a lower mass density than hard domains of the BD-based materials. The larger peak areas are attributed to slightly greater sample thicknesses. Comparison of IR spectra for an un-ionized material, HTPS-25-0.0, and the equivalent ionized sample, HTPS-25-5.0, shows that they are very similar. The bonded NH and C=O peaks of the ionized sample appear to be shifted very slightly to higher wavenumbers (higher energy).

C. Thermal Analysis

DSC curves for the BD- and MDEA-extended polymers are shown in Figures 4 and 5, respectively, and the thermal transition data are summarized in Table 2. The breadth of the soft domain glass transition provides a qualitative measure of soft phase homogeneity. For both the BD- and

MDEA-extended materials, the T_g of the siloxane was consistently 152 ± 1°K. This indicates that the poly(dimethylsiloxane)-polyurethane materials are highly phase separated. A T_g which does not shift with increasing hard segment content has been found in a series of polybutadiene polyurethanes (13) and polyisobutylene polyurethanes (14), which are also well phase separated.

All three samples in the butanediol chain-extended series showed a very small endotherm at about 337°K, which has been attributed to short-range ordering of the hard domains (27,28). The magnitude of the endotherm was about the same for all of the samples. Only sample HTPS-25, the BD-extended material with the highest hard segment content, showed significant hard segment crystallinity. This is an indication that for MDI/BD based polyurethanes there is a threshold in hard-segment volume fraction or average hard-segment length needed to obtain significant hard segment crystallinity. Because MDI/BD hard segments are crystallizable while those of MDI/MDEA are not, the hard domains in MDI/BD/HTPS materials are expected to have a higher mass density, especially when significant hard segment crystallinity exists, than the hard domains in MDI/MDEA/HTPS materials.

High temperature melting endotherms were not observed in the MDEA-extended poly(dimethylsiloxane)-polyurethane block copolymers. In the MDEA-extended polyurethanes, the methyl side group does not allow a sufficiently regular ordering of the hard segments to permit crystallization (15).

The results in Table 2 show that ion incorporation does not affect the soft domain glass transition temperature or the transition zone width of the MDEA-extended materials. This is due to the fact that the un-ionized materials are already highly phase separated. The un-ionized MDI/MDEA hard

segments show a small endotherm near 332°K. This endotherm has previously been reported as the hard domain T_g (15). After ionization, the endotherm at 332°K shifts to higher temperatures, and this shift is attributed to an alteration of the hard domains due to the formation of ionic aggregates or clusters.

D. Dynamic Mechanical Analysis

The results of dynamic mechanical experiments are displayed in Figures 6-9 and Table 3. In agreement with the DSC data, all the samples show a soft domain glass transition (E" peak, Figures 7 and 9) at approximately the same temperature. In the BD-extended series, a broadening in the β-peak and an enhancement of the rubbery modulus is observed as the hard segment content increases (Figure 6).

Figure 8 shows the storage modulus curves for the MDEA-extended series materials. In the un-ionized samples, as the hard segment concentration increases the β-peak broadens and the storage modulus increases. The ionized samples exhibit a higher rubbery modulus than the corresponding un-ionized samples, and a broad rubbery-plateau region develops. The plateau modulus increases with increasing ionization level. This suggests increased hard domain cohesion due to the aggregation of ionic groups, as the ionic groups provide inter-chain crosslinking within the hard domains. Ionization also slightly increases the hard domain volume fraction which causes an increase in the modulus due to a filler effect. Figure 9 also shows that ionization also produces a small secondary maximum (β_{max} in Table 3) in the loss modulus curve, suggesting that some disordering process takes place in the hard domains. This maximum shifts to higher temperatures with increasing ionic concentration, suggesting an enhanced domain cohesion at higher ionization levels.

E. Tensile Properties

Typical stress-strain curves for the BD- and MDEA-extended materials are shown in Figure 10, and the tensile properties are summarized in Table 4. Comparison of the BD-extended materials, HTPS-20 and HTPS-25, shows a higher Young's modulus and ultimate strength for the higher hard segment content material. By looking only at these two samples, it is impossible to determine whether the increased tensile strength is due to the effect of significant hard segment crystallinity or the effect of a higher hard domain volume fraction. A comparison of the tensile test results for HTPS-25 and HTPS-25-0.0 (BD-extended vs. MDEA-extended at almost the same hard segment content) settles this issue. The higher tensile strength of HTPS-25 (vs. HTPS-25-0.0) indicates that the presence of hard segment crystallinity is a more important factor in determining tensile properties than the hard segment volume fraction per se. Comparing the tensile test results of un-ionized (HTPS-25-0.0) and ionized (HTPS-25-5.0) MDEA-extended materials shows that ionic aggregation in hard domains also gives a material with a much higher tensile strength. These tensile test results lead directly to the important conclusion that hard domain cohesiveness, whether it is obtained via hard segment crystallinity or via ionic aggregation, is a much more important factor than hard domain volume fraction in determining the tensile properties of phase-separated block polyurethanes.

F. Small-Angle X-Ray Scattering

The desmeared small-angle x-ray scattering (SAXS) data are shown in Figures 11-13 and the characteristics of the scattering peaks are given in Table 5. The scattering curves show absolute intensity as a function of momentum transfer magnitude, q. The relation between q and the scattering

angle is $q = 4\pi \sin(\theta)/\lambda$ where λ is the x-ray wavelength and 2θ is the scattering angle.

The discussion of the SAXS data will be relatively qualitative. A more detailed analysis of the scattering data will be presented elsewhere. The SAXS discussion will focus on the following features of the intensity curves: (1) peak location which gives an indication of the interdomain distance, (2) peak height which is proportional to the contrast between phases, and (3) peak sharpness, as given by the full width at half maximum (FWHM) of the peak, which is a measure of the regularity in domain size or spacing. Features of the SAXS curves which are common to all four samples include: (1) a single prominent scattering peak, (2) an increase in intensity at the lowest scattering angles ($q < 0.2$ nm^{-1}), and (3) similar shapes of the curves at the highest scattering angles ($q > 1.0$ nm^{-1}).

SAXS curves of samples of different hard segment content but based on the same chain extender (BD) are shown in Figure 11. The scattering curves have the same shape, but the scattering peak for the sample with higher hard segment content is higher and is located at a smaller scattering angle. The increased peak height is primarily due to the presence of crystalline MDI/BD segments in the HTPS-25 sample, although the increased hard domain volume fraction also contributes to the increased peak height. Both samples have peaks with the same FWHM which indicates that the variation in hard domain size is the same. The increased long spacing for the sample with higher hard segment content could be due to the increased volume fraction of the hard domains in that material.

SAXS curves of samples with different chain extenders but the same hard segment content are shown in Figure 12. The flat peak top of

HTPS-25-0.0 is an artifact introduced by connecting data points with straight lines. The sample based on the MDEA chain extender has a much sharper peak, i.e. a smaller FWHM, which indicates that the hard domains in sample HTPS-25-0.0 are more uniform in size than those in the sample based on the BD chain extender (HTPS-25). The MDEA-extended sample also has a shoulder in the scattering curves at about $q = 0.85\ nm^{-1}$. This feature suggests more regular domain spacing (i.e. less local disorder). Based on the DSC results, the HTPS-25 (BD-extended) sample has significant hard segment crystallinity, but the HTPS-25-0.0 (MDEA-extended) sample does not. Thus, the hard domain mass density and electron density are greater for the BD-extended material. Therefore, the slightly higher SAXS peak and increased long spacing of the MDEA-extended sample indicates that its hard domain volume fraction (and thereby connectivity) is greater.

SAXS curves of the MDEA-extended samples before and after zwitterionization are shown in Figure 13. The increased peak height for the completely ionized sample (HTPS-25-5.0) is attributed to the aggregation of ionic groups so that the ionized hard domains have higher electron density. The increased long spacing for the completely ionized sample is probably due to its higher hard segment volume fraction. The level of ionization does not affect the peak sharpness as measured by the FWHM, which suggests that regularity in domain size is not affected by ionization. That is, the morphology of the polyurethane block polymer is not significantly affected by the incorporation of ionic groups into hard segments.

IV. CONCLUSIONS

On the basis of FTIR and DSC results poly(dimethylsiloxane)-polyurethane block polymers are highly phase-separated, as expected. The

presence of hard segment crystallinity and ionic functionality does not noticeably affect the phase separation. A high degree of phase separation is observed for both crystallizable and non-crystallizable hard segments. Thus, for polyurethane block polymers based on poly(dimethylsiloxane) soft segments the hard and soft domains are nearly completely phase separated and the phase separation is not significantly affected by the hard segment chemical structure or the hard segment content (for hard segment content in the range studied in this work).

Using MDEA as the hard segment extender instead of BD yields materials whose hard domains have (1) non-crystallizable hard segments, (2) lower mass density, (3) more uniform size, and (4) lower cohesion at the same hard segment content (assuming no ionization of the MDEA). The more uniform domain size for MDEA-extended materials, as indicated by SAXS, could be interpreted as being due to more chain folding in the hard domains of these materials, but without further evidence this should be viewed as a highly speculative conclusion.

For the MDEA-extended materials, ionic aggregation occurs after zwitterionization in solution followed by precipitation and spin casting. The ionic aggregation was deduced from solubility and SAXS results. Ionic aggregation explains the increased rubbery plateau modulus and tensile strength observed in zwitterionized materials.

On the basis of DSC, FTIR, and especially SAXS results, the hard segment crystallinity or ionic aggregation does not significantly change the sample morphology. That is, the morphology appears to be determined more by the extreme incompatibility of the poly(dimethylsiloxane) soft segments and the aromatic urethane hard segments than by the state of organization within the hard domains.

Reinforcement of the hard domains via hard segment crystallinity or via zwitterionization of the chain extender causes a dramatic increase in the Young's modulus, ultimate tensile strength, and rubbery plateau modulus of poly(dimethylsiloxane)-polyurethane segmented polymers. For the range of hard segment contents examined in this study, hard domain cohesion is more important than hard domain volume fraction in determining the tensile and viscoelastic properties of these elastomers.

ACKNOWLEDGEMENTS

The authors gratefully acknowledge partial financial support of this work by the Office of Naval Research and Naval Air Systems Command. We also wish to acknowledge partial support of this work by the Division of Materials Research of the National Science Foundation through Grant DMR-81-06888. One of the authors (Y.X.) wishes to acknowledge fellowship support from the Ministry of Education of the People's Republic of China.

REFERENCES

(1) G. M. Estes, S. L. Cooper and A. V. Tobolsky, J. Macromol. Sci.-Rev. Macromol. Chem., 4, 313 (1970).

(2) S. L. Aggarwal, ed., Block Polymers, Plenum Press, New York (1970).

(3) A. Noshay and J. E. McGrath, eds., Block Copolymers, Wiley, New York (1973).

(4) S. L. Cooper and G. M. Estes, eds., Multiphase Polymers, Adv. Chem. Ser., 176, American Chemical Society, Washington, D.C. (1979).

(5) N. S. Schneider, C. R. Desper, J. L. Illinger and A. O. King, J. Macromol. Sci.-Phys., B11, 527 (1975).

(6) P. E. Gibson, M. A. Vallance, and S. L. Cooper, in Developments in Block Copolymers (I. Goodman, ed.), Appl. Sci. Ser., Elsevier, London, 1982.

(7) A. Noshay and J. E. McGrath, Block Copolymers Overview and Critical Survey, Academic Press, New York (1977).

(8) W. Noll, Chemistry and Technology of Siloxanes, Academic Press, New York (1968).

(9) G. L. Gaines, Macromolecules, 14, 208 (1981).

(10) A. Braley, J. Macromol. Sci. Chem., A4, 529 (1970).

(11) R. S. Ward, Jr., and E. Nyilas, Organometallic Polymers, Academic Press, New York (1978).

(12) L. Le Duc, L. P. Blanchard, and S. L. Malhotra, J. Macromol. Sci., Chem., A14, 389 (1980).

(13) C. M. Brunette, S. L. Hsu, M. Rossman, W. J. MacKnight, and N. S. Schneider, Polym. Engr. and Sci., 21, 668 (1981).

(14) T. A. Speckhard, G. Ver Strate, P. E. Gibson and S. L. Cooper, Polym. Engr. and Sci., 23, 337 (1983).

(15) K. K. S. Hwang, C. Z. Yang, and S. L. Cooper, Polym. Engr. and Sci., 21, 1027 (1981).

(16) C. Z. Yang, K. K. S. Hwang, and S. L. Cooper, Macromol. Chem., 184, 651 (1983).

(17) T. A. Speckhard, K. K. S. Hwang, C. Z. Yang, W. R. Laupan, and S. L. Cooper, J. Macromol. Sci.-Phys., accepted for publication.

(18) J. A. Miller, K. K. S. Hwang, C. Z. Yang, and S. L. Cooper, J. Elast. and Plas., 15, 174 (1983).

(19) I. Yilgör, G. L. Wilkes, and J. E. McGrath, Polymer Preprints, 23, 286 (1982).

(20) O. Kratky, I. Pilz, and P. J. Schmitz, J. Colloid and Interface Sci., 21, 24 (1966).

(21) J. A. Lake, Acta. Cryst., 23, 191 (1967).

(22) S. W. Kantor, W. T. Grubb, and R. C. Osthoff, J. Amer. Chem. Soc., 76, 5190 (1954).

(23) C. S. P. Sung and N. S. Schneider, Macromolecules, 8, 68 (1975).

(24) C. B. Wang and S. L. Cooper, Macromolecules, 21, 11 (1983).

(25) S. L. Cooper, J. C. West, and R. W. Seymour, in Encyclopedia of Polymer Science and Technology, pp. 521, Wiley, New York (1978).

(26) V. W. Srichatrapimuk and S. L. Cooper, J. Macromol. Sci.-Phys., B15, 207 (1978).

(27) J. A. Miller, K. K. S. Hwang, and S. L. Cooper, J. Macromol. Sci.-Phys., B22, 321 (1983).

(28) J. W. C. Van Bogart, D. A. Bluemke, and S. L. Cooper, Polymer, 22, 1428 (1981).

Table 1

Material Characterizaion

Sample	Molar Ratio MDI/BD/HTPS (2000)				Molecular weight*	MDI wt %
HTPS-10	1	0	1		7.7×10^4	11.0
HTPS-20	2	1	1		4.6×10^4	19.3
HTPS-25	3	2	1		6.8×10^4	25.6
	MDI/MDEA/HTPS (2000)/1,3-PS					
HTPS-20-0	2	1	1	0	9.2×10^4	19.1
HTPS-20-3.0**	2	1	1	1		18.2
HTPS-25-0	3	2	1	0	7.7×10^4	25.0
HTPS-25-5.0**	3	2	1	2		23.2

* Determined in THF by GPC $\bar{M}_{peak}$

** Wt % SO_3 added during synthesis

Table 2

DSC Results

Material	Soft Segment		Hard Segment	
	T_g (°K)	Transition zone width (°K)	small endotherms (°K)	large endotherms (°K)
HTPS-10	153	6	337	-
HTPS-20	153	6	337,390,462,483	-
HTPS-25	152	7	337,380	462
HTPS-20-0	152	7	322	-
HTPS-20-3.0	152	8	355	-
HTPS-25-0	152	7	324	-
HTPS-25-5.0	152	7	384	-

Table 3

Dynamic Mechanical Results

Sample	E'' peak (°C)	β peak (°C)	Plateau Region (°C)		
			onset	end	width
HTPS-20	-124	-	-75	40	115
HTPS-25	-124	126	-75	50	125
HTPS-20-0.0	-124	95	-75	10	85
HTPS-20-3.0	-124	188	-75	150	225
HTPS-25-0.0	-124	113	-75	50	125
HTPS-25-5.0	-124	>200	-75	190	265

Table 4

Tensile Properties

Sample	Young's Modulus (MPa)	Ultimate Stress (MPa)	Elongation at Break %
HTPS-20	0.4	2.4	175
HTPS-25	1.8	5.0	171
HTPS-20-0	0.2	3.1	248
HTPS-25-0	0.3	3.4	270
HTPS-25-5.0	1.1	8.6	153

Table 5

SAXS Peak Characteristics

Sample	Hard Segment Weight Fraction	Peak Location (nm^{-1})	Peak FWHM (nm^{-1})	Long Spacing (nm)
HTPS-20	0.24	0.51	0.26	11.4
HTPS-25	0.33	0.46	0.26	12.6
HTPS-25-0.0	0.34	0.42	0.14	14.4
HTPS-25-5.0	0.39	0.39	0.13	15.6

Note: Long spacing was calculated from peak in Lorentz-corrected scattering curves, i.e. $q^2I(q)$.

Figure Captions

Figure 1 Relative viscosity vs. time for equilibration of one mole of 1,3-bis(4-hydroxybutyl)-tetramethyldisiloxane with six moles of D_4 with 0.1% $(CH_3)_4NOH$ at 80°C

Figure 2 Infrared spectra of HTPS-20

Figure 3 Infrared spectra of HTPS-10, HTPS-25, HTPS-25-0 and HTPS-25-5.0 in the NH and C=O stretching regions

Figure 4 DSC curves for the BD-extended series

Figure 5 DSC curves for the MDEA-extended series

Figure 6 Storage modulus E' and tan δ curves for the BD-extended series

Figure 7 Loss modulus E" curves for the BD-extended series

Figure 8 Storage modulus E' and tan δ curves for the MDEA-extended series

Figure 9 Loss modulus E" curves for the MDEA-extended series

Figure 10 Stress-strain curves for the BD- and MDEA-extended series

Figure 11 Desmeared SAXS curves for HTPS-20 and HTPS-25

Figure 12 Desmeared SAXS curves for HTPS-25 and HTPS-25-0.0

Figure 13 Desmeared SAXS curves for HTPS-25-0.0 and HTPS-25-5.0

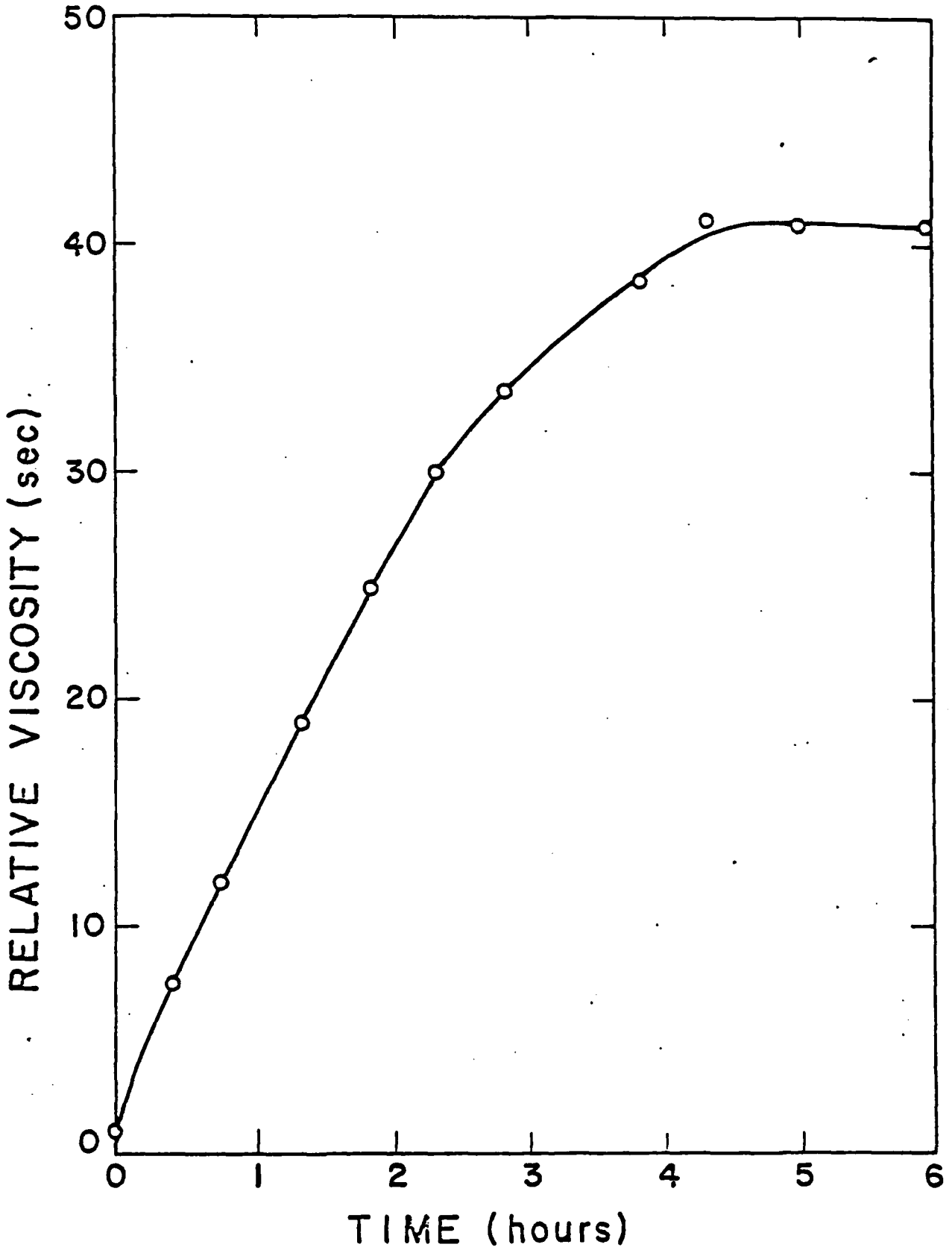
RELATIVE VISCOSITY (sec)
50
40
30
20
10
0
0
1
2
3
4
5
6
TIME (hours)

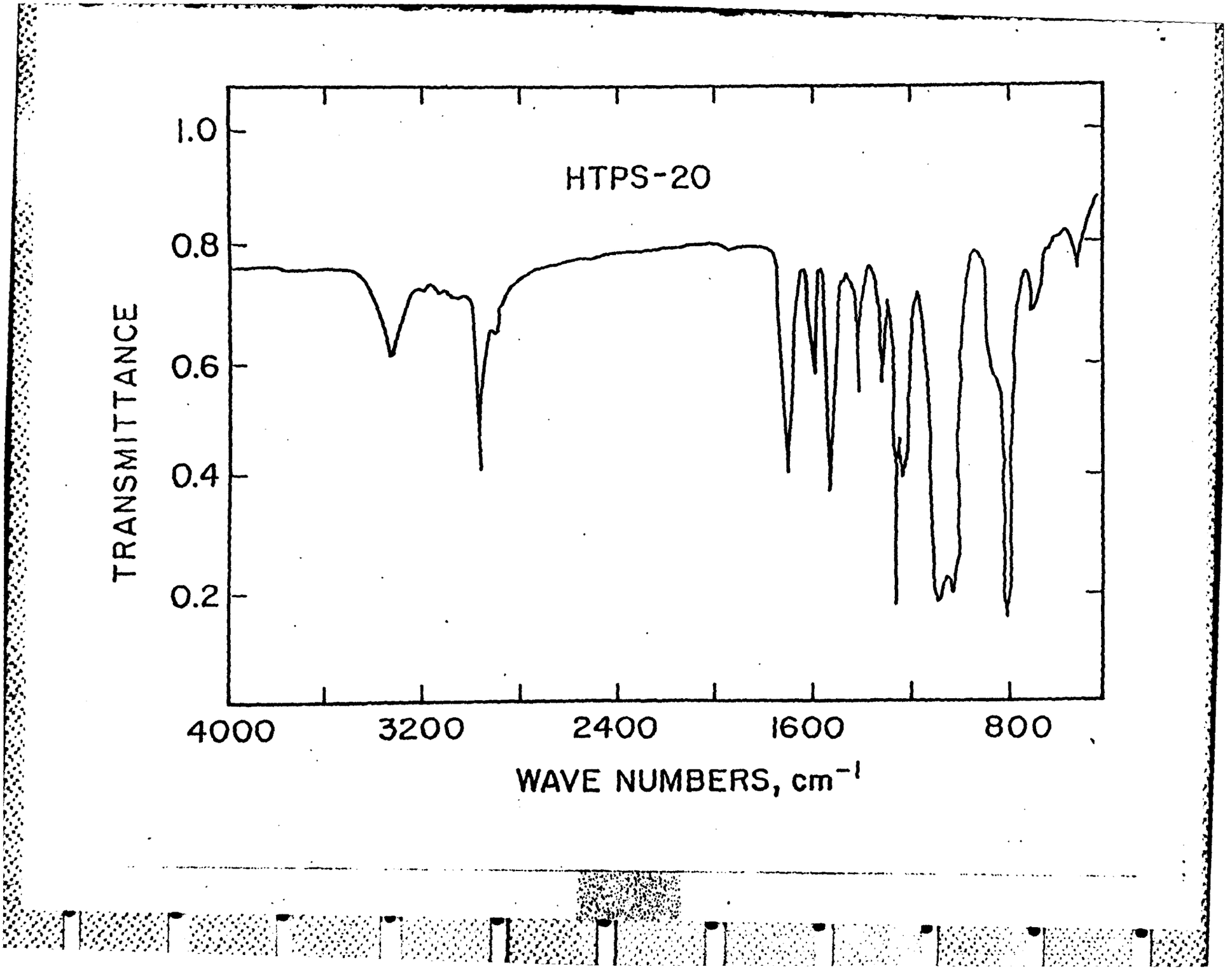
HTPS-20
TRANSMITTANCE
1.0
0.8
0.6
0.4
0.2
4000
3200
2400
1600
800
WAVE NUMBERS, cm⁻¹

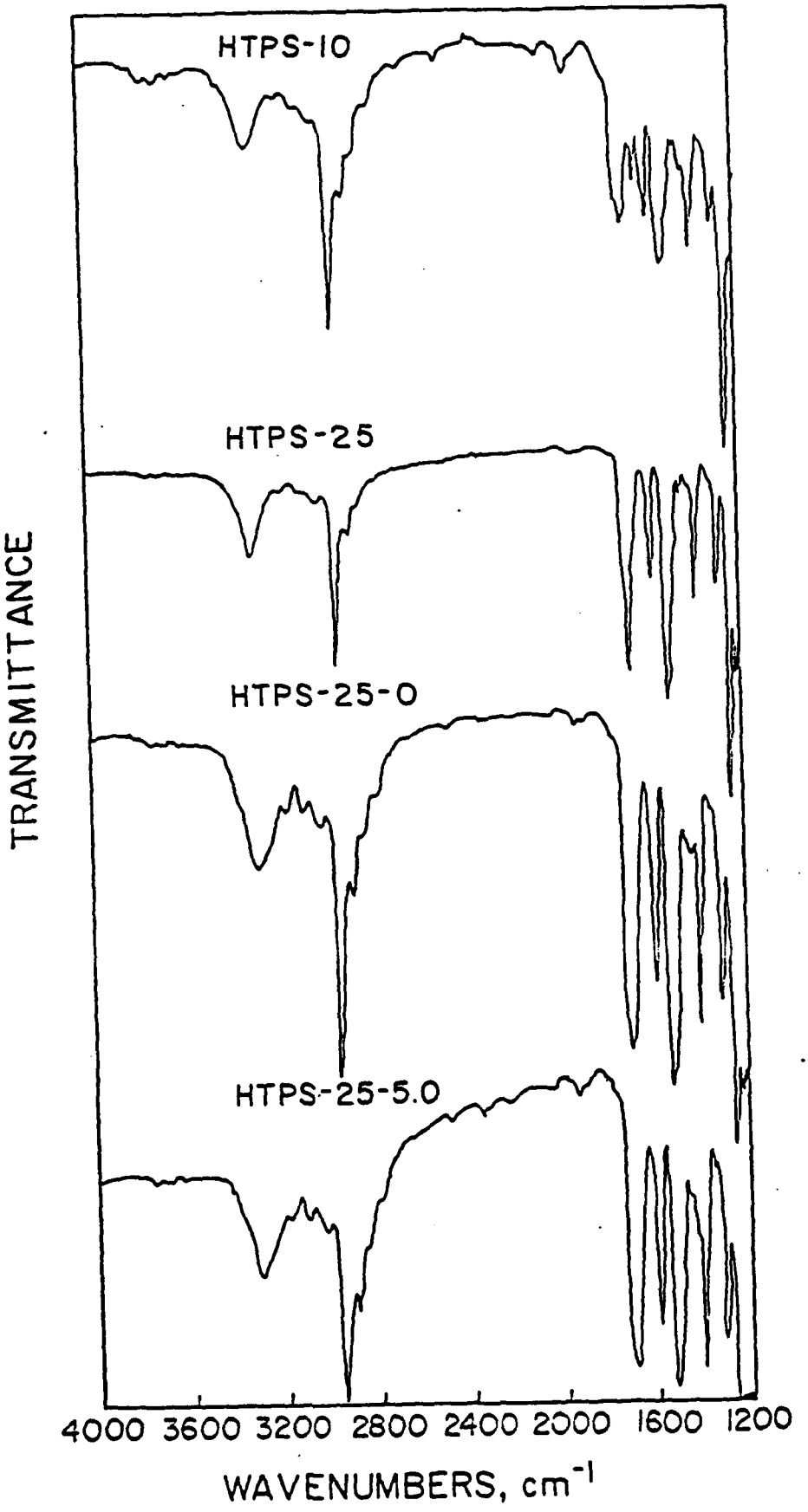
HTPS-10
HTPS-25
HTPS-25-0
HTPS-25-5.0
TRANSMITTANCE
4000 3600 3200 2800 2400 2000 1600 1200
WAVENUMBERS, cm-1

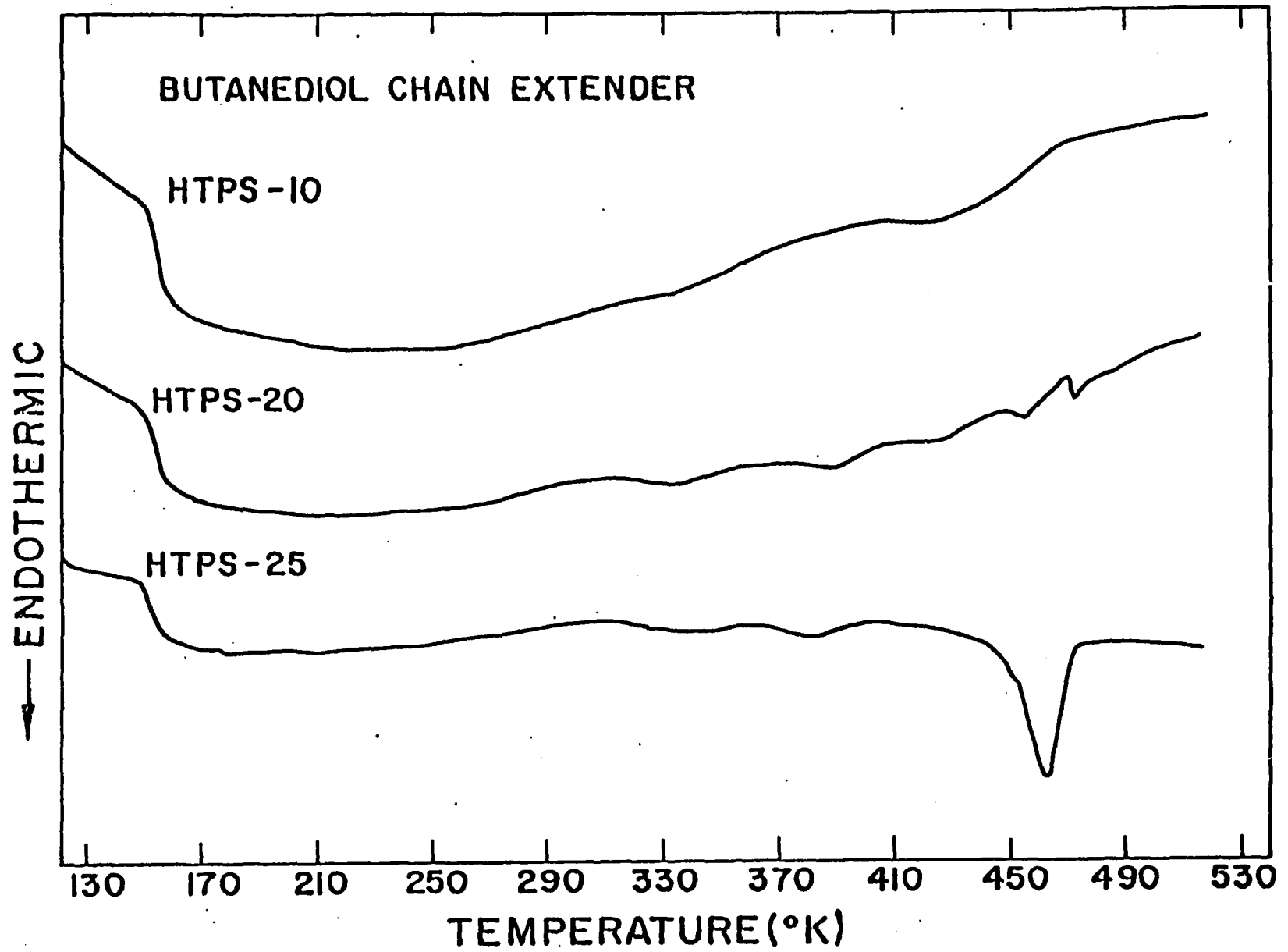
BUTANEDIOL CHAIN EXTENDER
HTPS-10
HTPS-20
HTPS-25
ENDOTHERMIC
130
170
210
250
290
330
370
410
450
490
530
TEMPERATURE(°K)

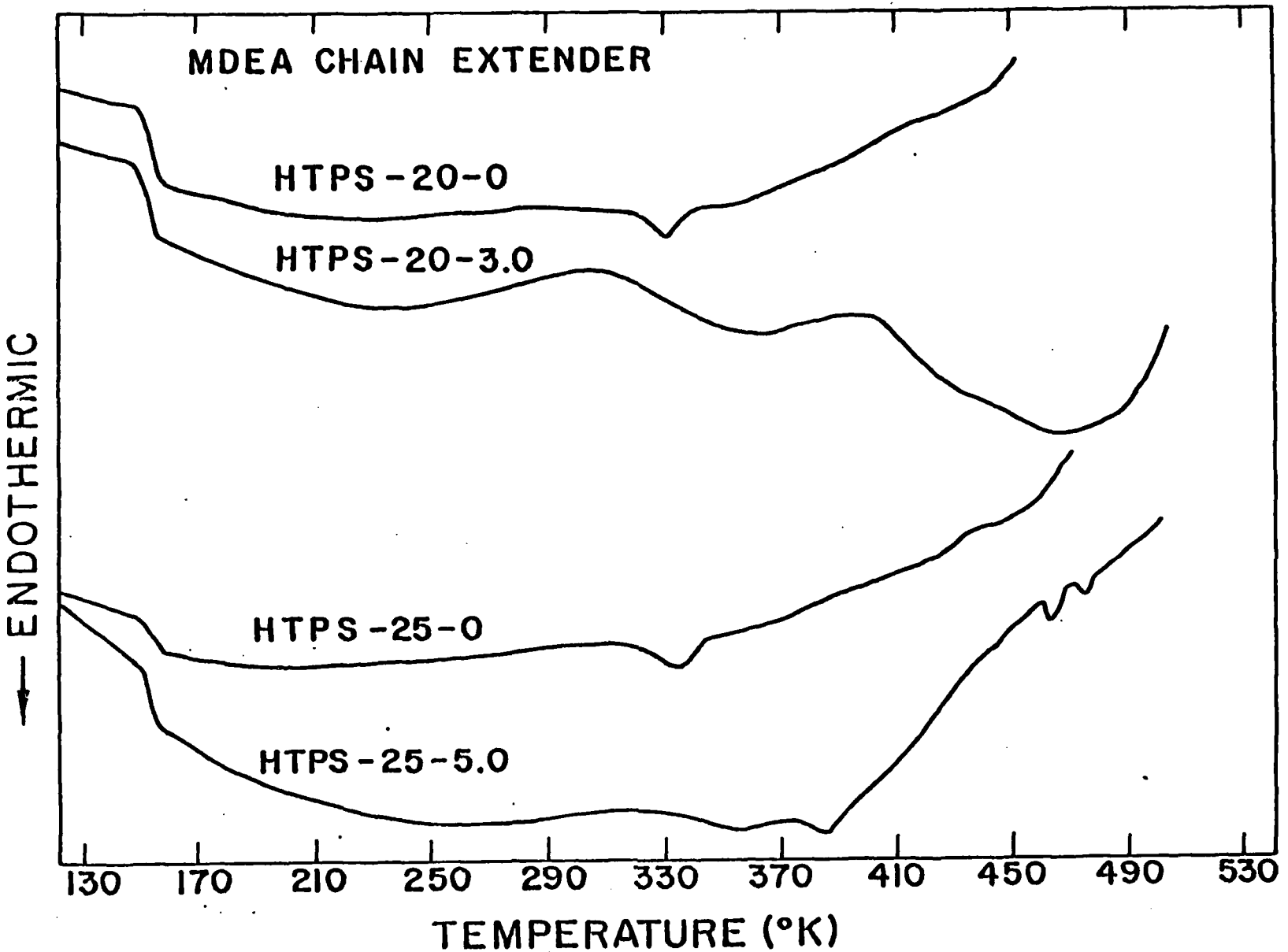
MDEA CHAIN EXTENDER
HTPS-20-0
HTPS-20-3.0
HTPS-25-0
HTPS-25-5.0
ENDOTHERMIC
130
170
210
250
290
330
370
410
450
490
530
TEMPERATURE (°K)

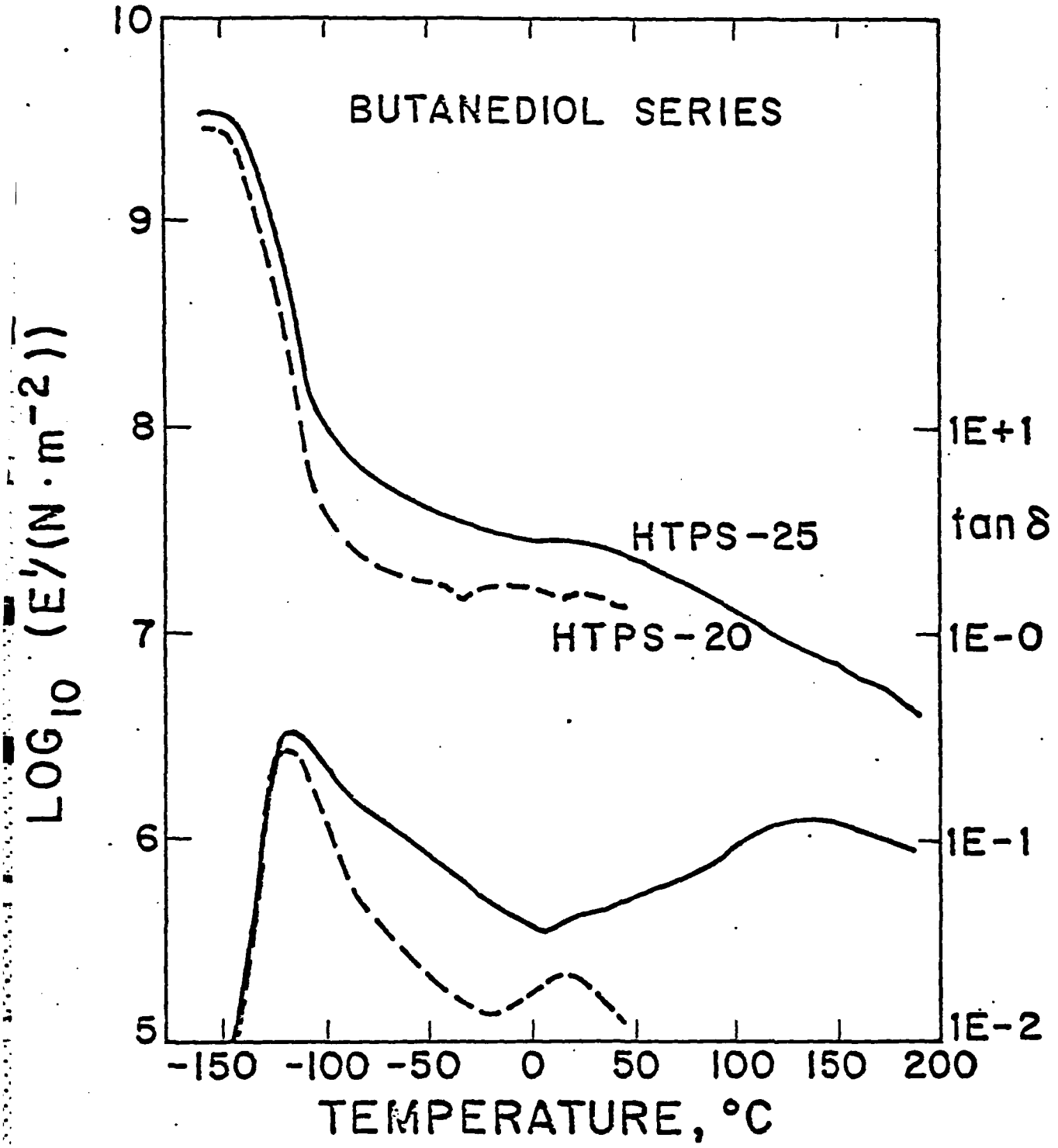
BUTANEDIOL SERIES
HTPS-25
HTPS-20
10
9
8
7
6
5
1E+1
1E-0
1E-1
1E-2
tan δ
LOG10 (E'/(N·m-2))
-150 -100 -50 0 50 100 150 200
TEMPERATURE, °C

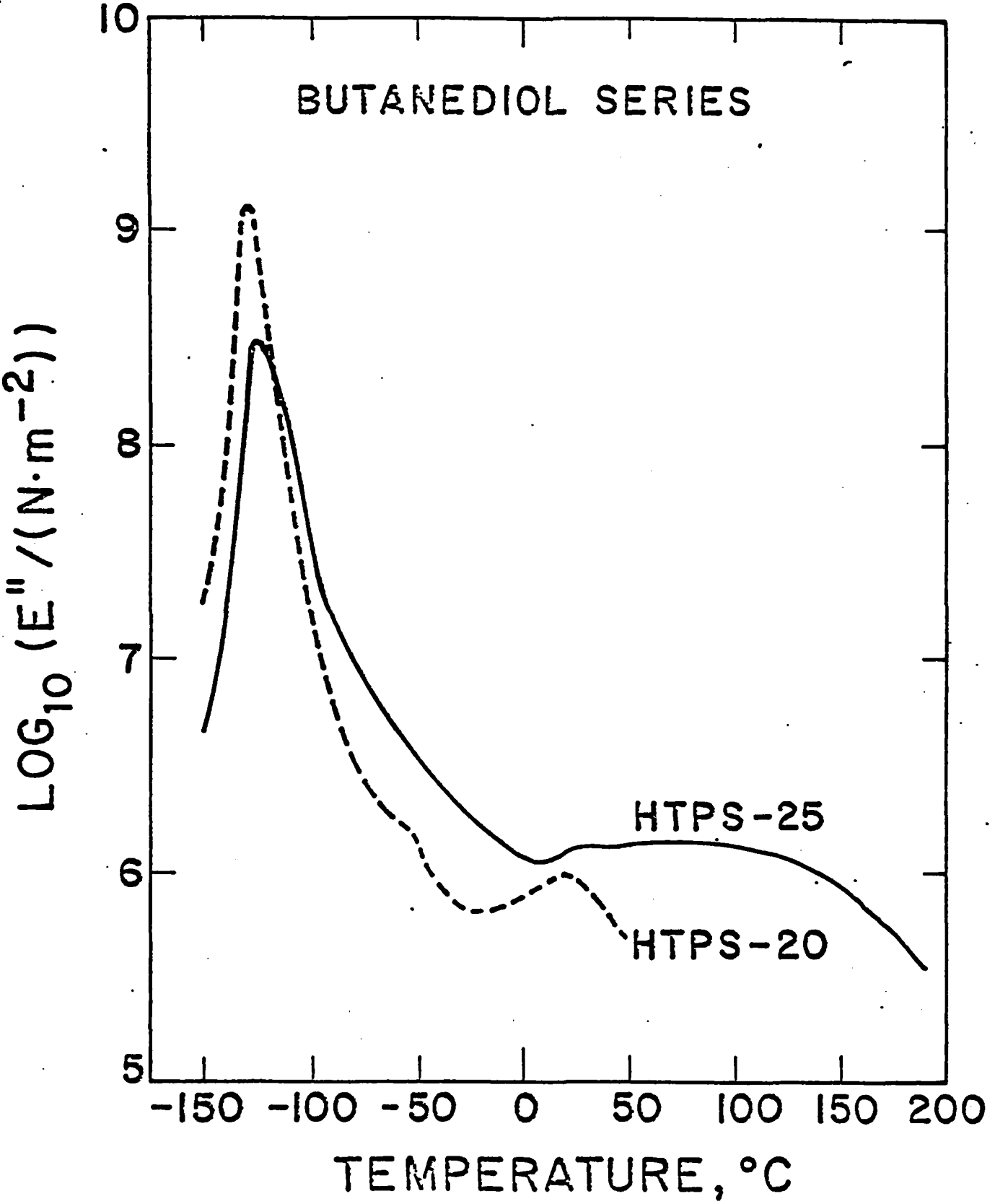
BUTANEDIOL SERIES
10
9
8
7
6
5
$LOG_{10}(E''/(N\cdot m^{-2}))$
HTPS-25
HTPS-20
-150 -100 -50 0 50 100 150 200
TEMPERATURE, °C

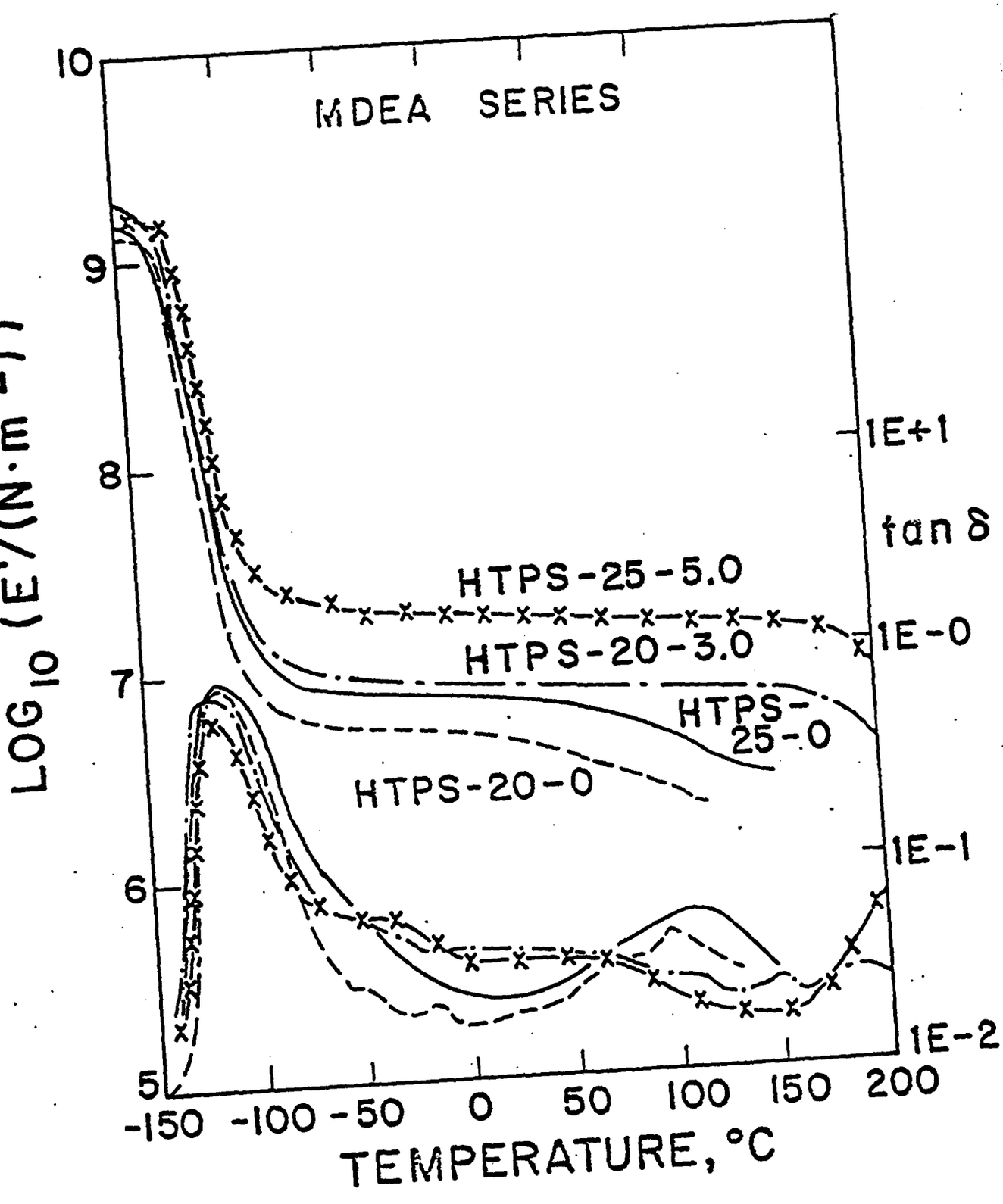
MDEA SERIES
HTPS-25-5.0
HTPS-20-3.0
HTPS-25-0
HTPS-20-0
LOG10 (E'/(N·m-2))
tan δ
TEMPERATURE, °C
10
9
8
7
6
5
1E+1
1E-0
1E-1
1E-2
-150
-100
-50
0
50
100
150
200

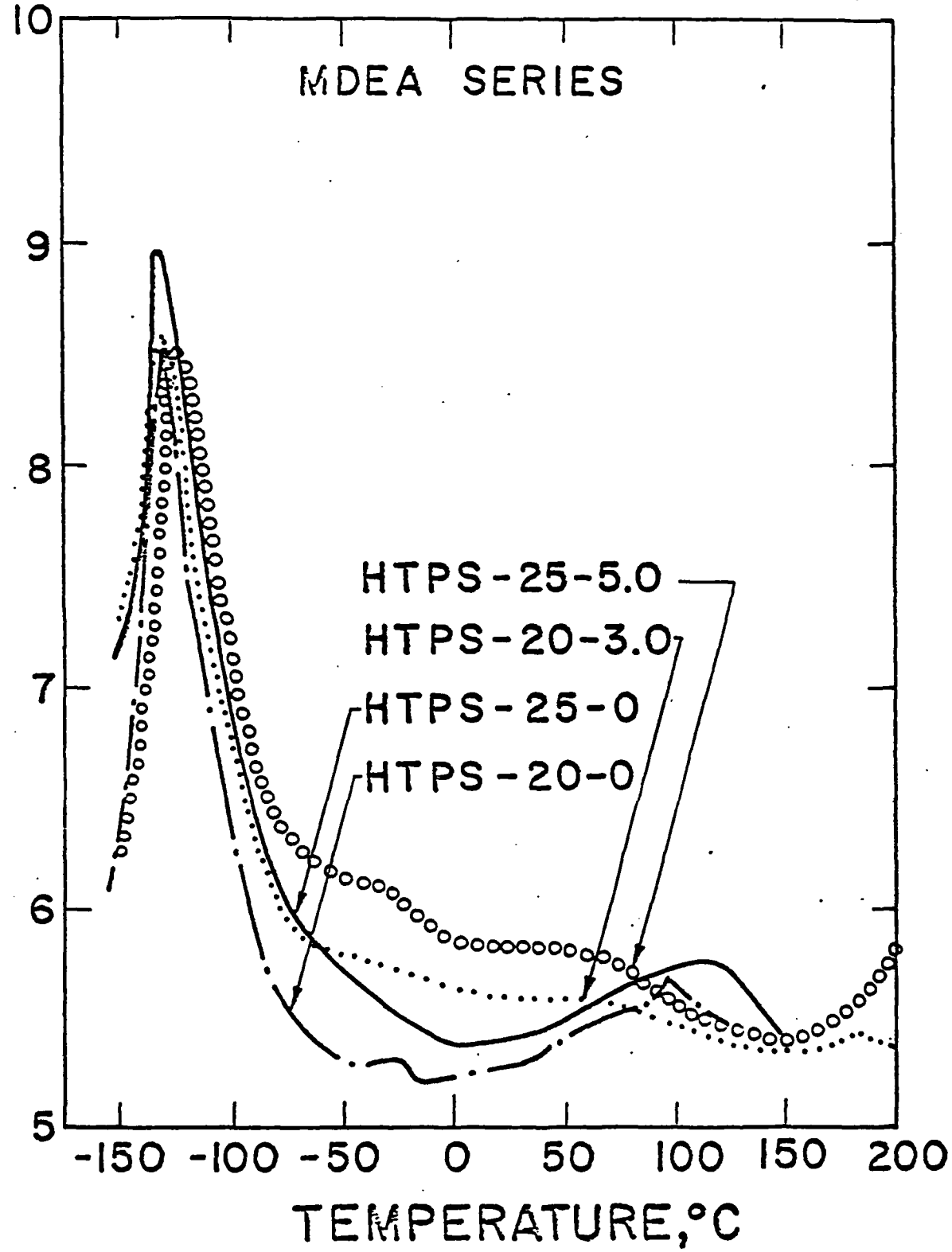
MDEA SERIES
HTPS-25-5.0
HTPS-20-3.0
HTPS-25-0
HTPS-20-0
10
9
8
7
6
5
-150
-100
-50
0
50
100
150
200
TEMPERATURE,°C
LOG10 (E''/(N·m⁻²))

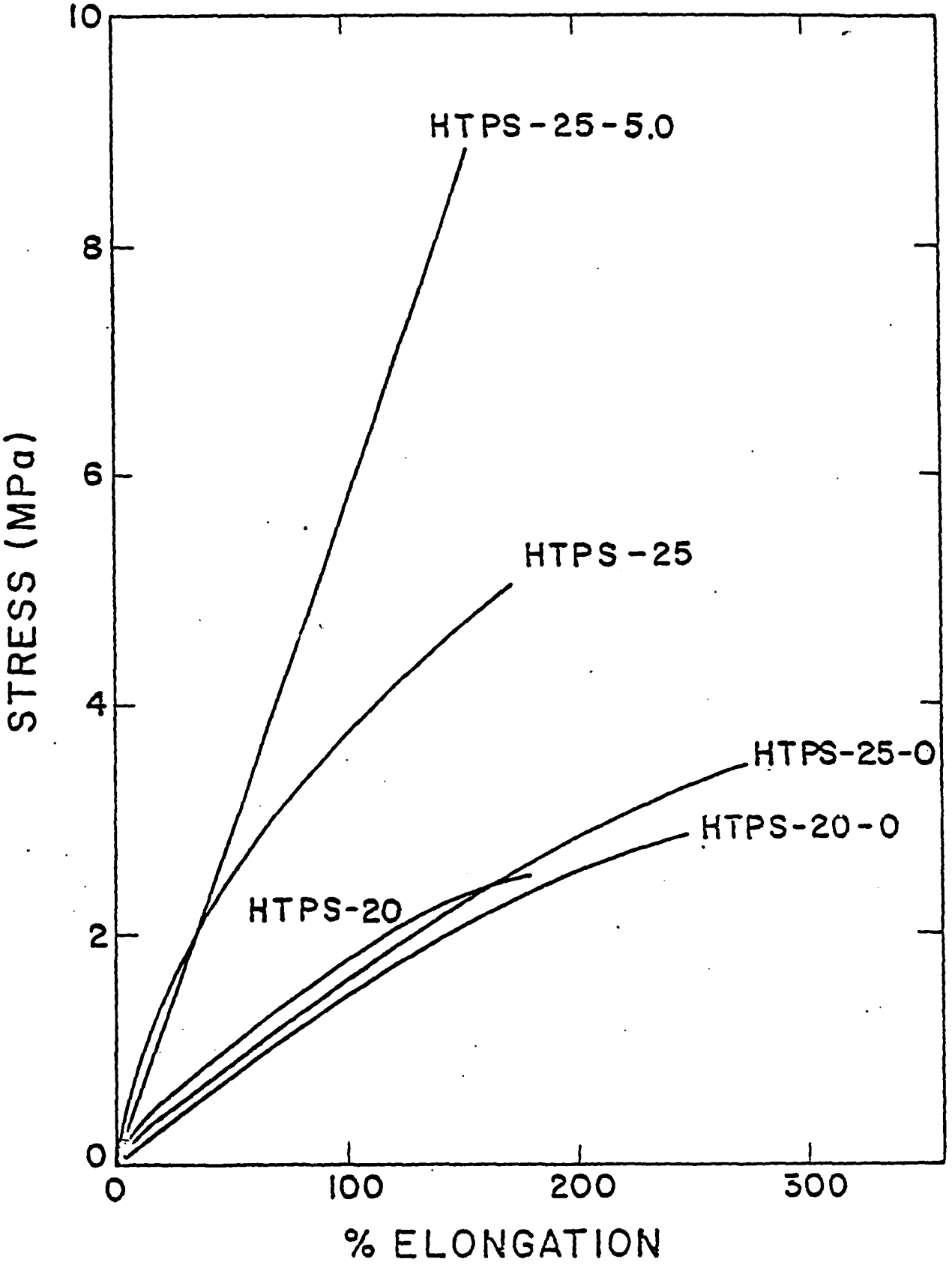
HTPS-25-5.0
HTPS-25
HTPS-25-0
HTPS-20-0
HTPS-20
STRESS (MPa)
% ELONGATION
0
2
4
6
8
10
0
100
200
300

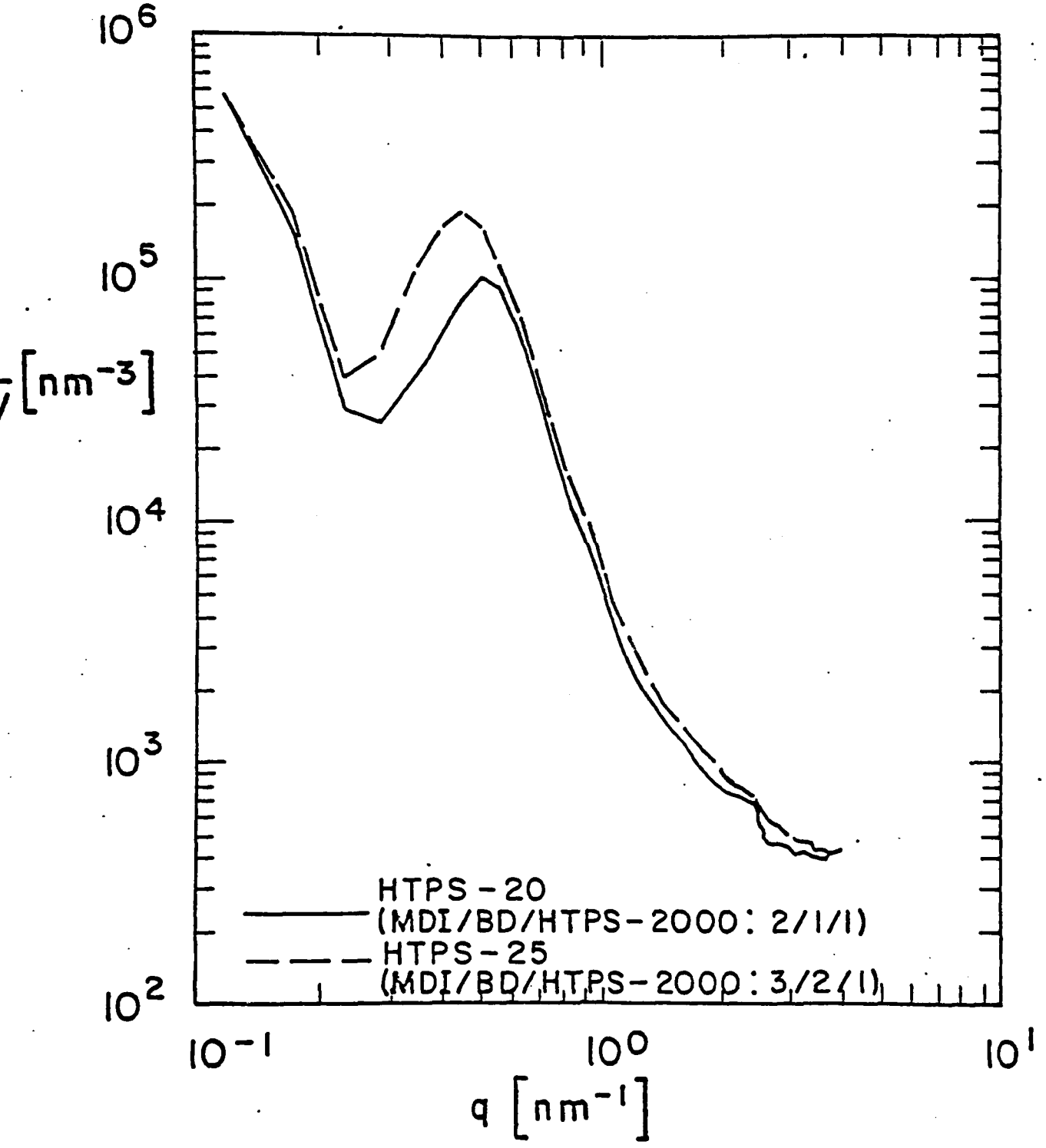
10^6
10^5
10^4
10^3
10^2
$\frac{I}{V}$ [nm^{-3}]
HTPS-20
(MDI/BD/HTPS-2000: 2/1/1)
HTPS-25
(MDI/BD/HTPS-2000: 3/2/1)
10^{-1}
10^0
10^1
q [nm^{-1}]

END

FILMED

1-85

DTIC